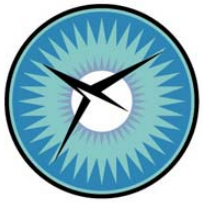

**NATIONAL INSTITUTE OF AEROSPACE**

**Final Report For:**

**NASA # NNL04AA06T**
**TM: Abedin Nurul**

# Characterization and Modeling of Indium Gallium Antimonide Avalanche Photodiode and of Indium Gallium Arsenide Two-band Detector

**Prepared by:**
**Old Dominion University**

**Reporting Period: Feb 2006**

# Report-February 2006
# Optical properties of AlGaAsSb and GaInAsSb alloys in the 0.01-6.0 eV region

## Introduction

A model of the optical properties of $Al_xGa_{1-x}As_ySb_{1-y}$ and $In_xGa_{1-x}As_ySb_{1-y}$ is presented, including the refractive, extinction, absorption and reflection coefficients in terms of the optical dielectric function of the materials. Energy levels and model parameters for each binary compound are interpolated to obtain the needed ternaries and quaternaries for various compositions. Bowing parameters are considered in the interpolation scheme to take into account the deviation of the calculated ternary and quaternary values from experimental data due to lattice disorders. The inclusion of temperature effects is currently being considered.

## Linear Interpolation Scheme

The quaternary material $A_xB_{1-x}C_yD_{1-y}$ is constructed of four binary compounds: AC, AD, BC, and BD; or else of four ternary compounds: $A_xB_{1-x}C$, $A_xB_{1-x}D$, $AC_yD_{1-y}$ and $BC_yD_{y-1}$.

In particular, for AlGaAsSb with form $A_xB_{1-x}C_yD_{1-y}$, its binary compounds are AC = AlAs; AD = AlSb; BC = GaAs; BD = GaSb. Its ternary compounds are ABC = AlGaAs; ABD = AlGaSb ; ACD = AlAsSb; BCD = GaAsSb.

Considering GaInAsSb with form $A_xB_{1-x}C_yD_{1-y}$, the binary compounds are AC = InAs; AD = InSb; BC = GaAs; BD = GaSb. The ternary compounds are: ABC = InGaAs; ABD = InGaSb ; ACD = InAsSb; BCD = GaAsSb.

The material parameters for ternary semiconductors (T) in the form $A_xB_{1-x}C$ are obtained from the linear interpolation of the transition parameters of the binary materials (B) (Vegard's rule) as follows [1, 2]:

$$T_{ABC}(x) = xB_{AC} + (1-x)B_{BC} - x(1-x)C_T, \qquad (1)$$

where $C_T$ is the bowing constant . Table I below gives the bowing parameters used in the calculation of the cutoff energy $E_0$ for each ternary.

**Table I**.
Bowing parameters used in the linear interpolation of the energy level $E_0$ for each ternary compound of AlGaAsSb and InGaAsSb [2].

| | $C_0$ (eV) |
|---|---|
| AlAsSb | 0.72 |
| GaAsSb | 1.2 |
| InAsSb | 0.596 |
| AlGaAs | 0.438 |
| GaInAs | 0.4 |
| AlGaSb | 0.47 |
| GaInSb | 0.413 |

Once the interpolation of the ternary parameters is known, the quaternary parameters (Q) for the lower energy levels (alloy in the form $A_xB_{1-x}C_yD_{1-y}$) are obtained from [1, 2]:

$$Q_{ABCD}(x,y) = \frac{1}{x(1-x)+y(1-y)}\left\{x(1-x)[yT_{ABC}(x)+(1-y)T_{ABD}(x)]+y(1-y)[xT_{ACD}(y)+(1-x)T_{BCD}(y)]\right\} \quad (2)$$

The quaternary material parameters (form $A_xB_{1-x}C_yD_{1-y}$) may also be obtained from the binary parameters using Vegard's rule [1, 2]:

$$Q_{ABCD}(x,y) = xyB_{AC} + x(1-y)B_{AD} + (1-x)yB_{BC} + (1-x)(1-y)B_{BD} + C_{A-B}x(1-x) + C_{C-D}y(1-y) \quad (3)$$

In the above expression, bowing parameters are assumed to arise from independent anion and cation sublattice disorders. Table II below gives the bowing parameters used in Eq. 3

**Table II**
Bowing parameters used in the linear interpolation of model parameters of the binary compounds of AlGaAsSb and InGaAsSb [2].

| | GaInAsSb (InGaAsSb) | | AlGaAsSb | |
|---|---|---|---|---|
| | $C_{A-B}$ | $C_{C-D}$ | $C_{A-B}$ | $C_{C-D}$ |
| $\Gamma_0[E_0/(E_0+\Delta_0)]$ (eV) | 0.65 | 1.14 | 2.83 | 5.28 |
| $E_1$ (eV) | -0.90 | 0.79 | -0.13 | 15.16 |
| $B_1$ | -2.18 | 2.88 | -1.71 | -20.02 |
| $B_2$ | -4.31 | -12.28 | -12.01 | 4.39 |
| $\Gamma_1[E_1+\Delta_1]$ (eV) | -7.01 | -9.66 | -0.52 | -12.16 |
| D | -8.89 | -5.81 | -72.98 | -7.38 |
| $\Gamma[Eg^{ID}]$ (eV) | -7.01 | -9.66 | -0.52 | -12.16 |

## Semi-empirical Model of the Optical Dielectric Function

Using the model developed by S. Adachi [3-6] and extended in [7, 8], the contributions from the energy levels to the real and imaginary parts of the dielectric function of III-V binaries with a zinc-blende type structure are approximated with the equations detailed below. The parameters are interpolated using Eq. (1). Adding all individual contributions gives the real and imaginary parts of the dielectric function.

$$\varepsilon(\nu) = \varepsilon_{1\infty} + \varepsilon^{I}(\nu) + \varepsilon^{II}(\nu) + \varepsilon^{III}(\nu) + \varepsilon^{IV}(\nu). \tag{4}$$

Contribution from the $E_0(\Gamma)$ / $[E_0(\Gamma) + \Delta_0(\Gamma)]$ energy gap

These transitions are from the 3D $M_0$ critical points (CPs). Assuming parabolic bands, the contributions from the $E_0$ and $E_0 + \Delta_0$ transitions to the real and imaginary parts of the dielectric function, labeled $\varepsilon_{1,a}$ and $\varepsilon_{2,a}$, respectively, are given by:

$$\varepsilon^{I}(\nu) = AE_0^{-1.5}\left( f\left(\frac{h\nu + i\Gamma}{E_0}\right) + \frac{1}{2}\left(\frac{E_0}{E_0 + \Delta_0}\right)^{1.5} \cdot f\left(\frac{h\nu + i\Gamma}{E_0 + \Delta_0}\right)\right), \tag{5}$$

where

$$f(z) = z^{-2}\left(2 - (1+z)^{0.5} - (1-z)^{0.5}\right). \tag{6}$$

A is a strength parameter dependent on the reduced mass and the squared momentum matrix element and $\Gamma$ accounts for a lifetime broadening.

Contribution from the $E_1(\Lambda)$ / $[E_1(\Lambda)+\Delta_1(\Lambda)]$ transition

These transitions are from the 3D $M_1$ CPs. Their contribution to the dielectric function, labeled $\varepsilon_b$, can be treated as a 2D minima $M_0$:

$$\varepsilon^{II}(\nu) = -B_1\left(\frac{h\nu + i\Gamma}{E_1}\right)^{-2} \ln\left(1 - \left(\frac{h\nu + i\Gamma}{E_1}\right)^{2}\right) - B_2\left(\frac{h\nu + i\Gamma}{E_1 + \Delta_1}\right)^{-2} \ln\left(1 - \left(\frac{h\nu + i\Gamma}{E_1 + \Delta_1}\right)^{2}\right), \tag{7}$$

$\Gamma$ accounts for a lifetime broadening. $B_1$ and $B_2$ are strength parameters given by:

$$B_1 = 44\frac{E_1 + \frac{\Delta_1}{3}}{a_0 E_1^{\,2}}, \tag{8}$$

$$B_2 = 44\frac{E_1 + \frac{2\Delta_1}{3}}{a_0 (E_1 + \Delta_1)^2}, \tag{9}$$

where $a_0$ is the lattice constant, assumed here independent of temperature. The above equations for $B_1$ and $B_2$, while not as accurate as fitted parameters, are functions of energy and therefore more physically sound, allowing the introduction of external perturbations to the model, such as temperature, pressure variation, etc. To increase accuracy, they have been assigned constant values.

The discrete series of exciton lines at the $E_1$ / $E_1 + \Delta_1$ critical points are given by

$$\varepsilon^{III}(\nu) = \sum_{n=1}^{+\infty} \frac{1}{(2n-1)^3} \left( \frac{B_{1x}}{E_1 - [G_1/(2n-1)^2] - h\nu - i\Gamma_1} + \frac{B_{2x}}{E_1 + \Delta_1 - [G_{1s}/(2n-1)^2] - h\nu - i\Gamma_1} \right), \tag{10}$$

where $B_{1x}$ , $B_{2x}$ are strength parameters and $G_1$ , $G_{1s}$ are the Rydberg energy of the $E_1$, $E_1 + \Delta_1$ excitons, assumed to be zero.

Contribution from the $E_0$'($\Gamma$), $E_2$(X) and $E_2$($\Sigma$) gap

Since these transitions do not correspond to any well-defined critical point, they are characterized by three damped harmonic oscillators (i.e., j = 1, 2, 3 for $E_0$'($\Gamma$), $E_2$(X) and $E_2$($\Sigma$) ):

$$\varepsilon^{IV}(\nu) = \sum_{j=1}^{3} \frac{C_{E_j} E_j^2}{E_j^2 - (h\nu)^2 - ih\nu\Gamma_{E_j}}, \tag{11}$$

where $C_{Ej}$ and $\Gamma_{Ej}$ are, respectively, the nondimensional (i.e., constant) strength and broadening parameters.

Contribution from the indirect band-gap $E_g^{ID}$

The transition in this band-gap is expressed as a 2nd order process in the perturbation, giving:

$$\varepsilon^{V}(\nu) = \frac{2D}{\pi} \left\{ -\frac{\left(E_g^{ID}\right)^2}{(h\nu + i\Gamma)^2} \ln\left(\frac{E_c}{E_g^{ID}}\right) + \frac{1}{2}\left(1 + \frac{E_g^{ID}}{h\nu + i\Gamma}\right)^2 . \ln\left(\frac{h\nu + i\Gamma + E_c}{h\nu + i\Gamma + E_g^{ID}}\right) \right.$$
$$\left. + \frac{1}{2}\left(1 - \frac{E_g^{ID}}{h\nu + i\Gamma}\right)^2 \ln\left(\frac{h\nu + i\Gamma - E_c}{h\nu + i\Gamma - E_g^{ID}}\right) \right\}. \tag{12}$$

Here, D is the indirect gap strength parameter independent of the photon energy, $\Gamma$ introduces a phenomenologic damping, and $E_c$ is a high-energy cutoff, assumed equal to $E_1$, which prevents nonphysical parabolic bands extending to infinite energies. $\varepsilon_{1,d}$ and $\varepsilon_{2,d}$ are the real and imaginary parts of $\varepsilon_d(\nu)$.

Frequency dependent Gaussian damping

As suggested in [7], the damping constants $\Gamma_i$ in Adachi's model are replaced with the following expression derived in [9]:

$$\Gamma_i'(\nu) = \Gamma_i \exp\left[ -\alpha_i \left( \frac{h\nu - E_i}{\Gamma_i} \right)^2 \right], \tag{13}$$

where $\alpha_i$ is an adjustable parameter. The above serves to eliminate the extended absorption tails in $\varepsilon_2$ caused by the Lorentzian line shape used for broadening in Adachi's model.

Table III below gives the parameters for the dielectric function equations for the various binary materials.

Once the dielectric function is determined, the real part of the complex refractive index n and its imaginary part k, called the extinction coefficient (or attenuation index) of the material, can be calculated using the following expressions [1, 3]:

$$n = \left( \frac{\left( \varepsilon_1^{\,2} + \varepsilon_2^{\,2} \right)^{1/2} + \varepsilon_1}{2} \right)^{1/2} \tag{14}$$

$$k = \left( \frac{\left( \varepsilon_1^{\,2} + \varepsilon_2^{\,2} \right)^{1/2} - \varepsilon_1}{2} \right)^{1/2} \tag{15}$$

The absorption coefficient ($\alpha$) and the normal incidence reflectivity ® are expressed in terms of n and k as follows [1, 3]:

$$R = \left| \frac{n - ik - 1}{n - ik + 1} \right|^2 = \frac{(n-1)^2 + k^2}{(n+1)^2 + k^2} \tag{16}$$

$$\alpha = \frac{4\pi k}{\lambda} \tag{17}$$

**Table III**. Basic parameters (at 300K) used in the calculation of the dielectric function of AlAs [10, 4, 7], AlSb [6, 8], InAs [3, 5], InSb [3, 5, 8], GaAs [10, 3, 4, 5, 7] and GaSb [3, 5, 8] for Adachi's model w/Gaussian broadening.

| Parameter | AlAs | AlSb | InAs | InSb | GaAs | GaSb |
|---|---|---|---|---|---|---|
| $E_0(\Gamma)$ (eV) | 2.993 | 2.27 | 0.36 | 0.18 | 1.410 | 0.72 |
| $E_0(\Gamma)+\Delta_0(\Gamma)$ (eV) | 3.201 | 2.99 | 0.76 | 0.99 | 1.746 | 1.46 |
| A ($eV^{1.5}$) | 14.21 | 29.0 | 0.61 | 0.19 | 3.97 | 0.71 |
| $\Gamma_0\,[E_0/(E_0+\Delta_0)]$ (eV) | 0.0107 | 0.015 | … | … | 0.039 | … |
| $\alpha_0\,[E_0/(E_0+\Delta_0)]$ | 1.617 | … | … | … | 1.65 | … |
| $E_1(\Lambda)$ (eV) | 3.888 | 2.84 | 2.50 | 1.80 | 2.926 | 2.05 |
| $E_1(\Lambda)+\Delta_1(\Lambda)$ (eV) | 4.087 | 3.23 | 2.78 | 2.30 | 3.170 | 2.50 |
| $a_0$ (Å) | 5.6611 | 6.1355 | 6.0583 | 6.479 | 5.65325 | 6.09593 |
| $B_1$ | 4.381 | | 6.59 | 6.37 | | |
| $B_2$ | 0.103 | | … | … | | |
| $B_{1x}$ (eV) | 0.639 | … | … | … | | … |
| $B_{2x}$ (eV) | 0.770 | … | … | … | | … |
| $\Gamma_1\,[E_1/(E_1+\Delta_1)]$ (eV) | 0.125 | 0.14 | 0.21 | 0.16 | 0.15 | 0.09 |
| $\alpha_1\,[E_1/(E_1+\Delta_1)]$ | 0.012 | … | … | … | 0.01 | … |
| $E_0'(\Gamma)$ (eV) | 4.660 | 3.70 | … | … | 4.49 | … |
| $C\,[E_0'(\Gamma)]$ | 0.0049 | 1.83 | … | … | 0.193 | … |
| $\Gamma\,[E_0'(\Gamma)]$ (eV) | 0.597 | 0.666 | … | … | 0.55 | … |
| $\alpha\,[E_0'(\Gamma)]$ | 0.281 | … | … | … | 0.060 | … |
| $E_2(X)$ (eV) | 4.710 | 4.05 | 4.45 | 3.9 | 4.74 | 4.0 |
| $C\,[E_2(X)]$ | 1.3552 | 1.23 | 1.78 | 5.37 | 0.269 | 5.69 |
| $\Gamma\,[E_2(X)]$ (eV) | 0.434 | 0.365 | 0.481 | 1.24 | 0.68 | 1.16 |
| $\alpha\,[E_2(X)]$ | 0.052 | … | … | … | 0.060 | … |
| $E_2(\Sigma)$ (eV) | 4.976 | … | … | … | 4.88 | … |
| $C\,[E_2(\Sigma)]$ | 0.8815 | … | … | … | 0.11 | … |
| $\Gamma\,[E_2(\Sigma)]$ (eV) | 0.414 | … | … | … | 0.26 | … |
| $\alpha\,[E_2(\Sigma)]$ | 0.023 | … | … | … | 0.060 | … |
| $E_g^{ID}$ * (eV) | … | 1.61 | 1.07 | 0.93 | … | 0.76 |
| D | … | 1.00 | 20.8 | 19.5 | … | 7.4 |
| $\Gamma\,[E_g^{ID}]$ (eV) | … | 0.040 | … | … | … | … |
| $\alpha\,[E_g^{ID}]$ | … | … | … | … | … | … |
| $\varepsilon_{1\infty}$ | 0.02 | … | 2.8 | 3.1 | 0.77 | 1.0 |

* $E_g^x(\Gamma_8^v \rightarrow X_6^c$ transitions)

Modeled parameters for each binary were verified with the reported data and models [4-10]. Quaternary alloy parameters obtained from the model, such as the refractive index, were compared to the experimental and calculated values in Ref. 1, and are in relatively good agreement with the experimental data over a wider frequency range.

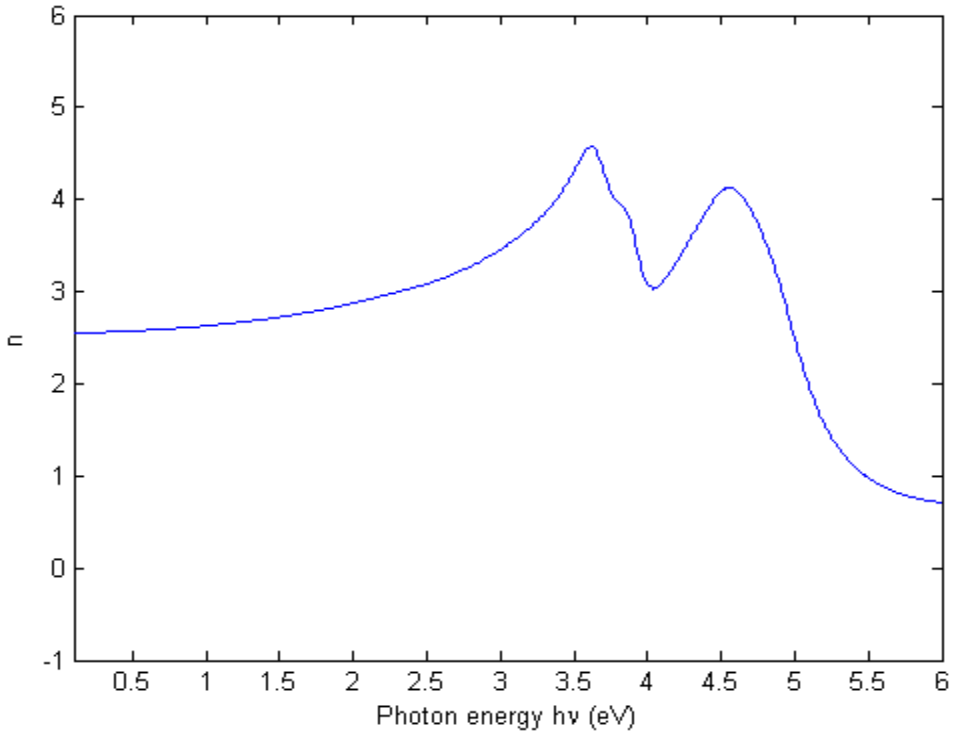


**Figure 1**. Refractive index of $Al_xGa_{1-x}As_ySb_{1-y}$ for x=0.8, y=1.

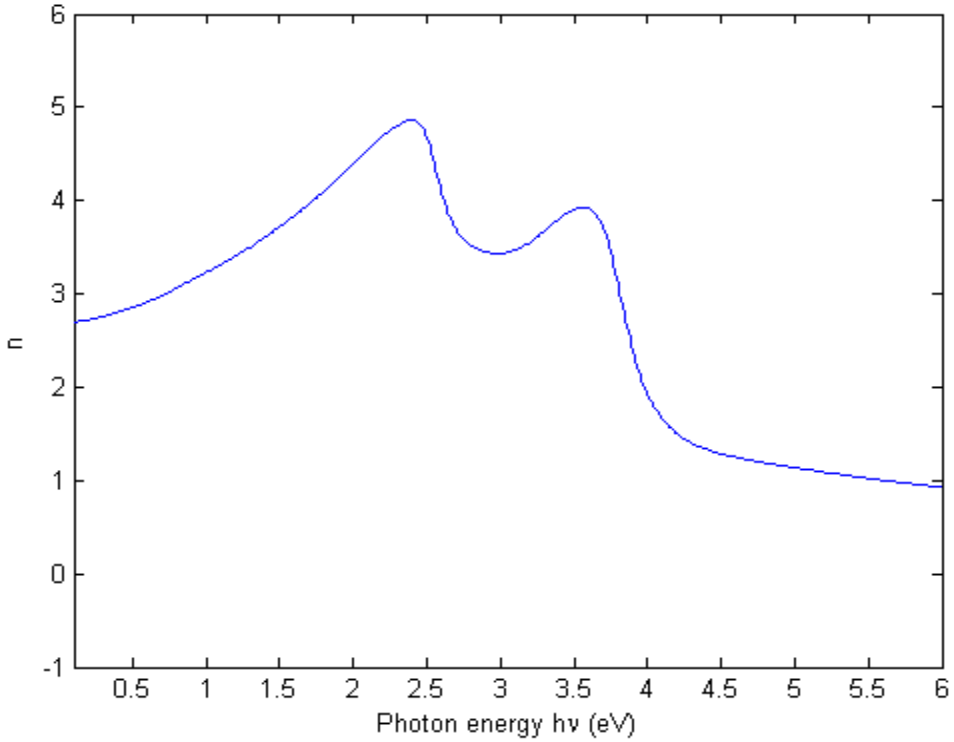


**Figure 2**. Refractive index of $Ga_xIn_{1-x}As_ySb_{1-y}$ for x=0.85, y=0.14.

**References**


[1] S. Adachi, “Physical properties of III-V semiconductor compounds: InP, InAs, GaAs, GaP, InGaAs, and InGaAsP,” Wiley (1992).

[2] M. Linnik, A. Christou, “Calculations of optical properties for quaternary III-V semiconductor alloys in the transparent region and above (0.2-4.0 eV),” *Physica B*, 318, 140-161 (2002).

[3] S. Adachi, “Model dielectric constants of GaP, GaAs, GaSb, InP, InAs, and InSb,” *Phys. Rev. B* **35**(14), 7454-7463 (1987).

[4] S. Adachi, “Optical properties of $Al_xGa_{1-x}As$ alloys,” *Phys. Rev. B*, **38**(17), 345-352, (1988).

[5] S. Adachi, “Optical dispersion relations for GaP, GaAs, GaSb, InP, InAs, InSb, $Al_xGa_{1-x}As$, and $In_{1-x}Ga_xAs_yP_{1-y}$,” *J. Appl. Phys*. **66**(12), 6030-6040 (1989).

[6] S. Adachi, “Optical dispersion relations for AlSb from E = 0 to 6.0 eV,” *J. Appl. Phys*. **67**(10), 6427-6431 (1990).

[7] A. D. Rakic and M. L. Majewski, “Modeling the optical dielectric function of GaAs and AlAs: Extension of Adachi’s model,” *J. Appl. Phys*., **80**(10) (1996).

[8] A.B. Djurisic, E.H. Li, D. Rakic, M.L. Majewski, “Modeling the optical properties of AlSb, GaSb, and InSb,” *Appl. Phys. A.*, **70**, 29-32, (2000).

[9] C.C. Kim, S. Sivananthan, “Modeling the optical dielectric function of II-VI compound CdTe,” *J. Appl. Phys.* **78**(6), 4003-4010 (1995).

[10] A. B. Djurisic, A. D. Rakic, P. C. K. Kwock, E. H. Li, M. L. Majewski, and J.M. Elazar, “Modeling the optical constants of $Al_xGa_{1-x}As$ alloys,” *J. Appl. Phys*., **86**(7), 445-451 (1999).